Supplementary Figure S1

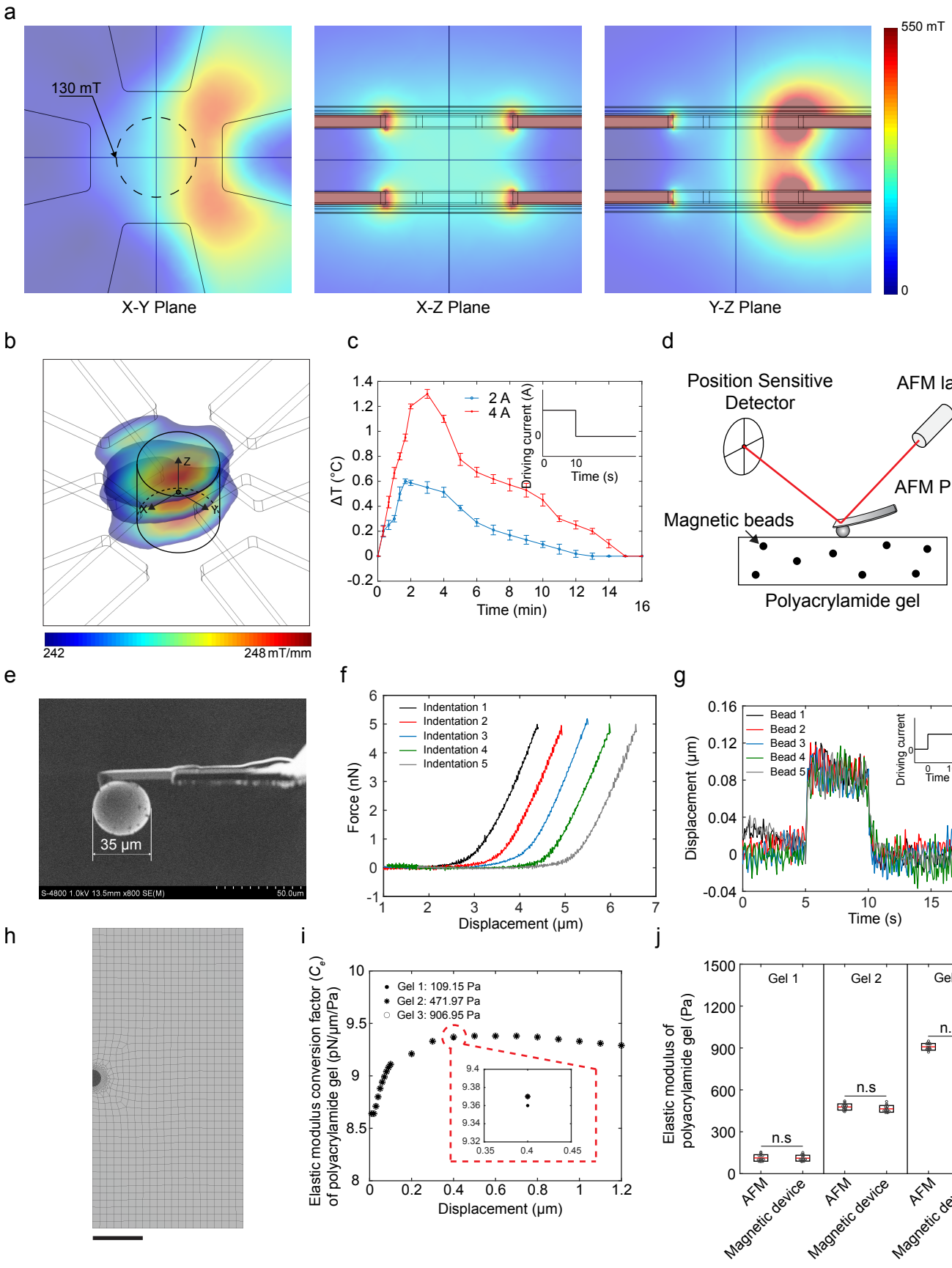

Figure S1. 3D magnetic device characterisation. a, Simulated magnetic field under 2 A actuation plotted in X-Y, X-Z and Y-Z planes as shown in Fig. 2c. The dashed line shows the boundary of the working space. Arrow indicates the minimum magnetic field in the working space. **b**, Simulated magnetic field gradient distribution in three different planes within the working space. **c**, Temperature change in the working space centre under 10 s of 2 A and 4 A actuation. **d**, Schematic represents AFM indentation of polyacrylamide (PA) gel containing magnetic beads. **e**, Scanning electron micrograph of an AFM cantilever with a spherical tip of 35 μm diameter. **f**, Representative AFM indentation (force-displacement) curves performed on the same PA gels that were >100 μm apart. **g**, Representative displacement-time curves of magnetic actuations performed on beads. Data shows five beads that were at least 100 μm apart. **h**, Axisymmetric mesh of finite element (FE) model. **i**, The elastic conversion factor of different gels at different displacements. **h**, Comparison of polyacrylamide gel with distinct elastic moduli measured by AFM and our magnetic device (15 measurements per gel on 3 gel samples). Error bars indicate s.d.. Scale bars represent 10 μm.

Supplementary Figure S2

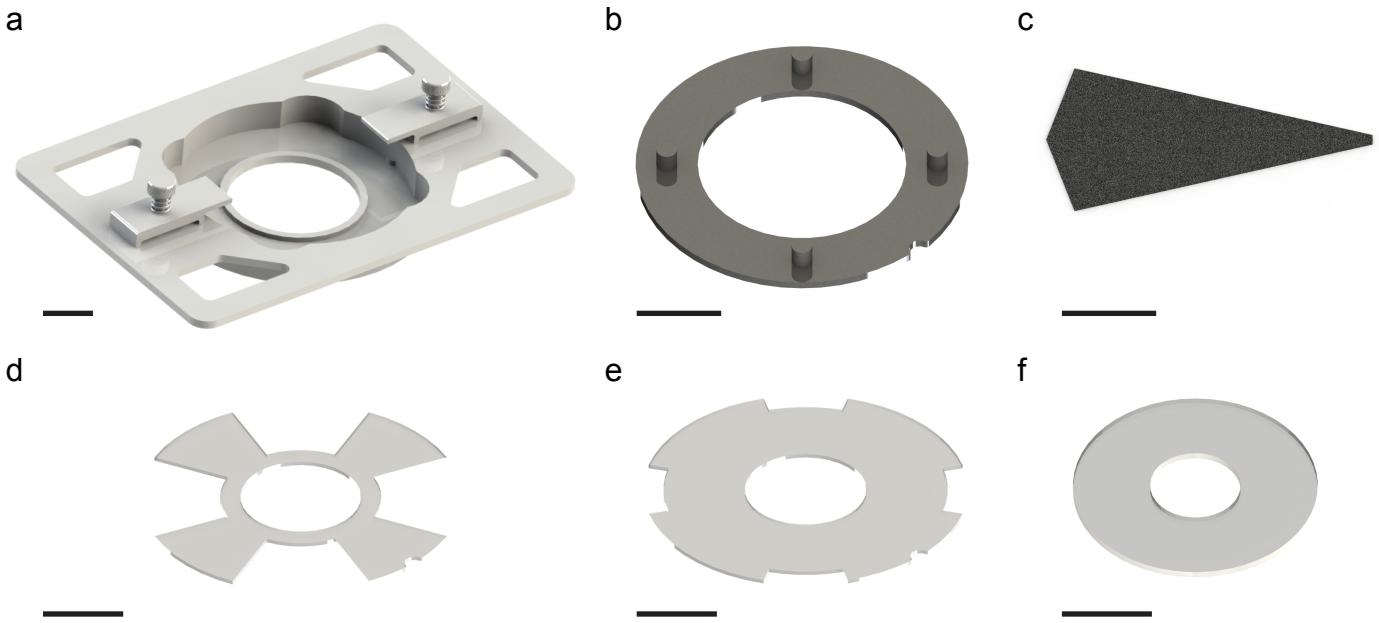

Figure S2. 3D magnetic device components. a-f, SolidWorks rendering of stage (a), magnetic yoke (b), magnetic pole (c), upper pole holder (d), bottom pole holder (e), imaging chamber (f). Scale bars represent 2 cm (a, b, d and e) and 1 cm (c and f).

Supplementary Figure S3

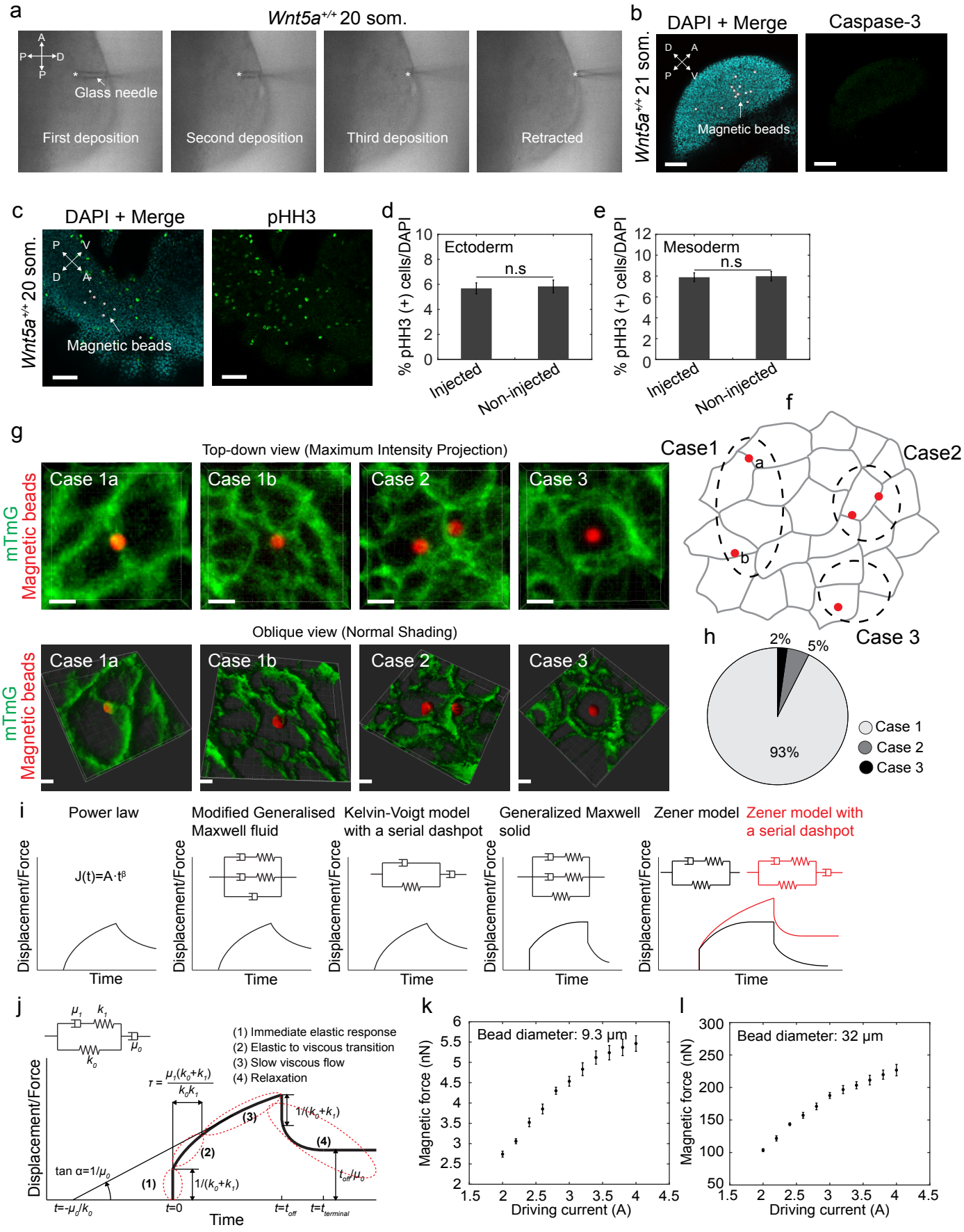

Figure S3. 3D tissue stiffness mapping using magnetic device. a, Step-wise microinjection of magnetic beads during retraction of the glass needle from the limb bud. Asterisks indicate the needle tip position. Micropipette tip diameter: 7 μm. **b**, Confocal image of injected mouse limb bud visualising DAPI (cyan), magnetic beads (red) and anti-caspase 3 immunostaining (green). **c**, Confocal image of injected mouse limb bud visualising DAPI (cyan) magnetic beads (red) and phospho-histone H3 (green). **d, e**, Histogram representing percentage of pHH3-positive cells in injected and non-injected mouse limb buds (ectoderm (d); mesoderm (e)). **f**, Illustration of bead positions inside tissue after microinjection. Case 1: bead successfully adhered to a cell membrane, on the outside (a) or on the inside (b) of cell membrane. Case 2: more than one bead adhered to a single cell or multiple beads ended up in too close a distance (e.g., one-cell distance). Case 3: bead trapped inside a cell. **g**, Top-down and oblique views of different bead positions corresponding to their illustrated positions shown in f, rendered by Maximum Intensity Projection and Normal Shading, respectively. **h**, Pie graph shows the percentage of different bead positions. **i**, Viscoelastic models that have been applied previously to quantify tissue properties and their displacement/force-time relations. Zener model with a serial dashpot best captured the viscoelastic properties that we observed in our experiments. **j,** Theoretical creep response and relaxation curve of the Zener model with a serial dashpot. **k, l**, Magnetic force-driving current calibration results for 9.3 and 32 μm magnetic beads. **m**, Magnetic beads of different sizes (first three panels) were injected into tissue (fourth and fifth panels) to compare results. Scale bars represent 100 μm (a-c), 10 μm (g), and 20 μm (m).

Supplementary Figure S4

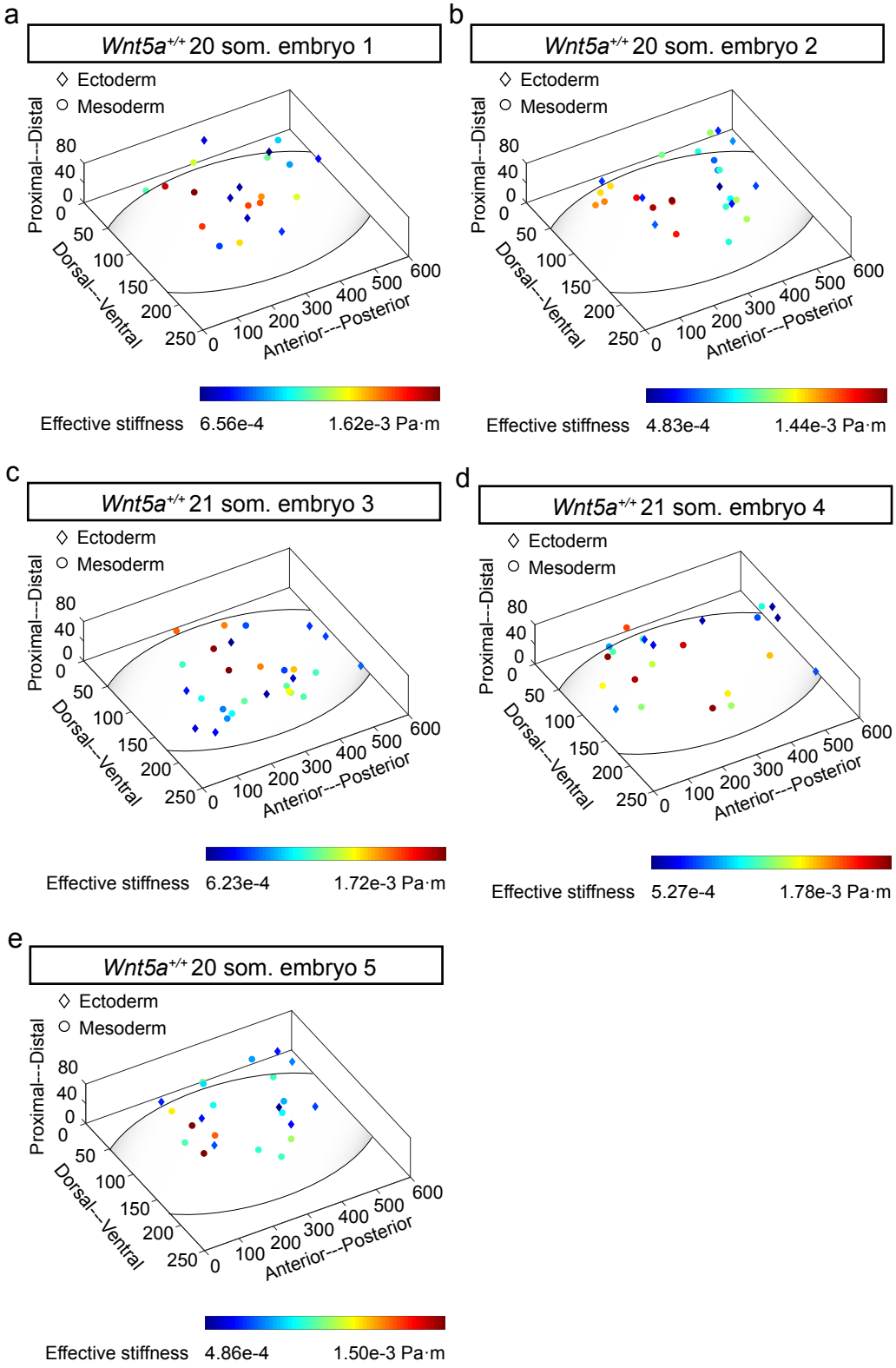

Figure S4. Non-normalised 3D tissue effective stiffness map. a-e, Non-normalised absolute effective stiffness maps of individual 20~21 somite stage WT limb buds.

Supplementary Figure S5

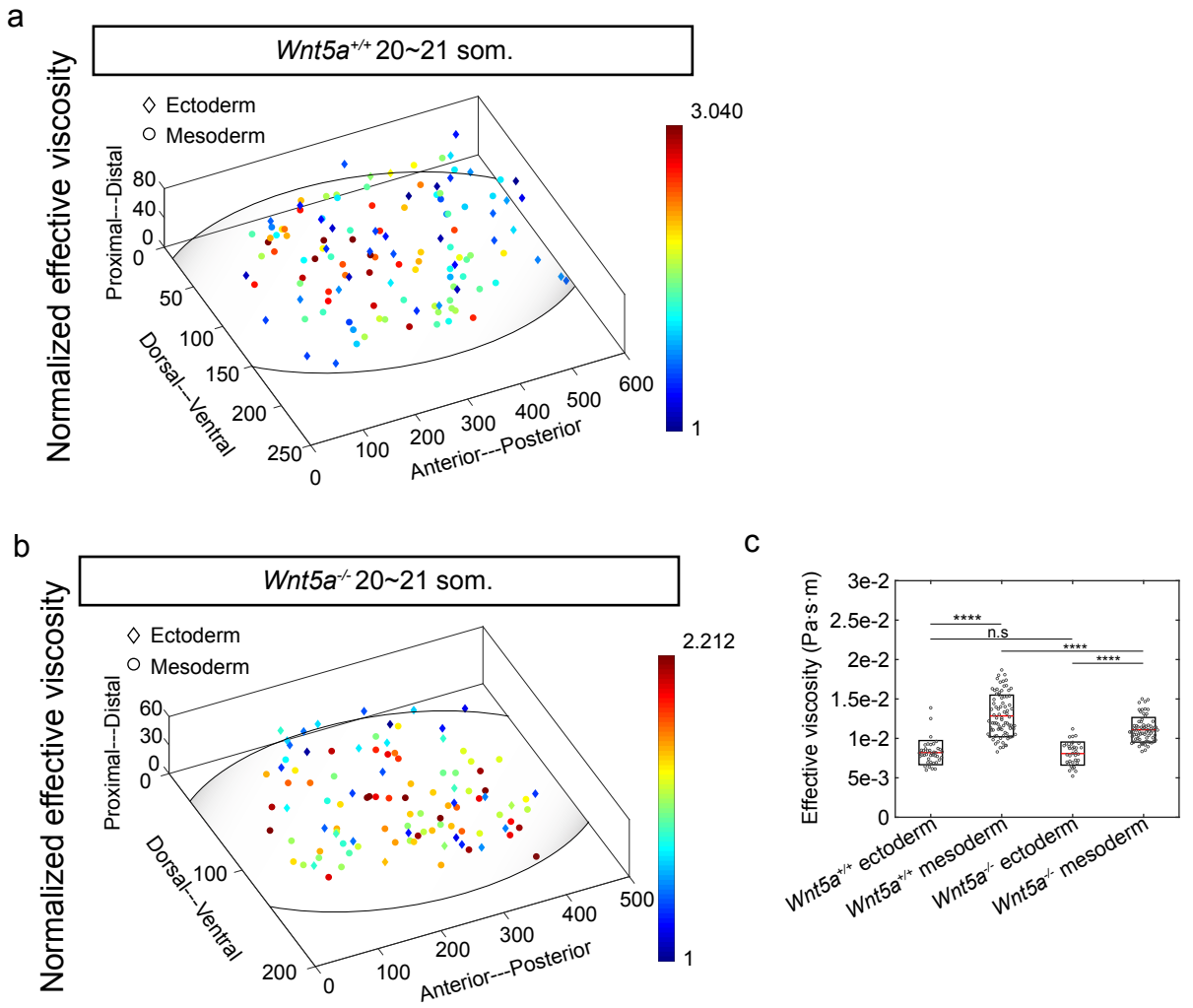

Figure S5. 3D tissue viscosity map. a, **b**, Normalised effective viscosity map of 20~21 somite stage WT (*n*=5 embryos) and *Wnt5a-/-* (*n*=4 embryos) limb buds. **c**, Absolute effective viscosity values of data shown in a and b (two-tailed *t*-test, ****p<0.0001).

Supplementary Figure S6

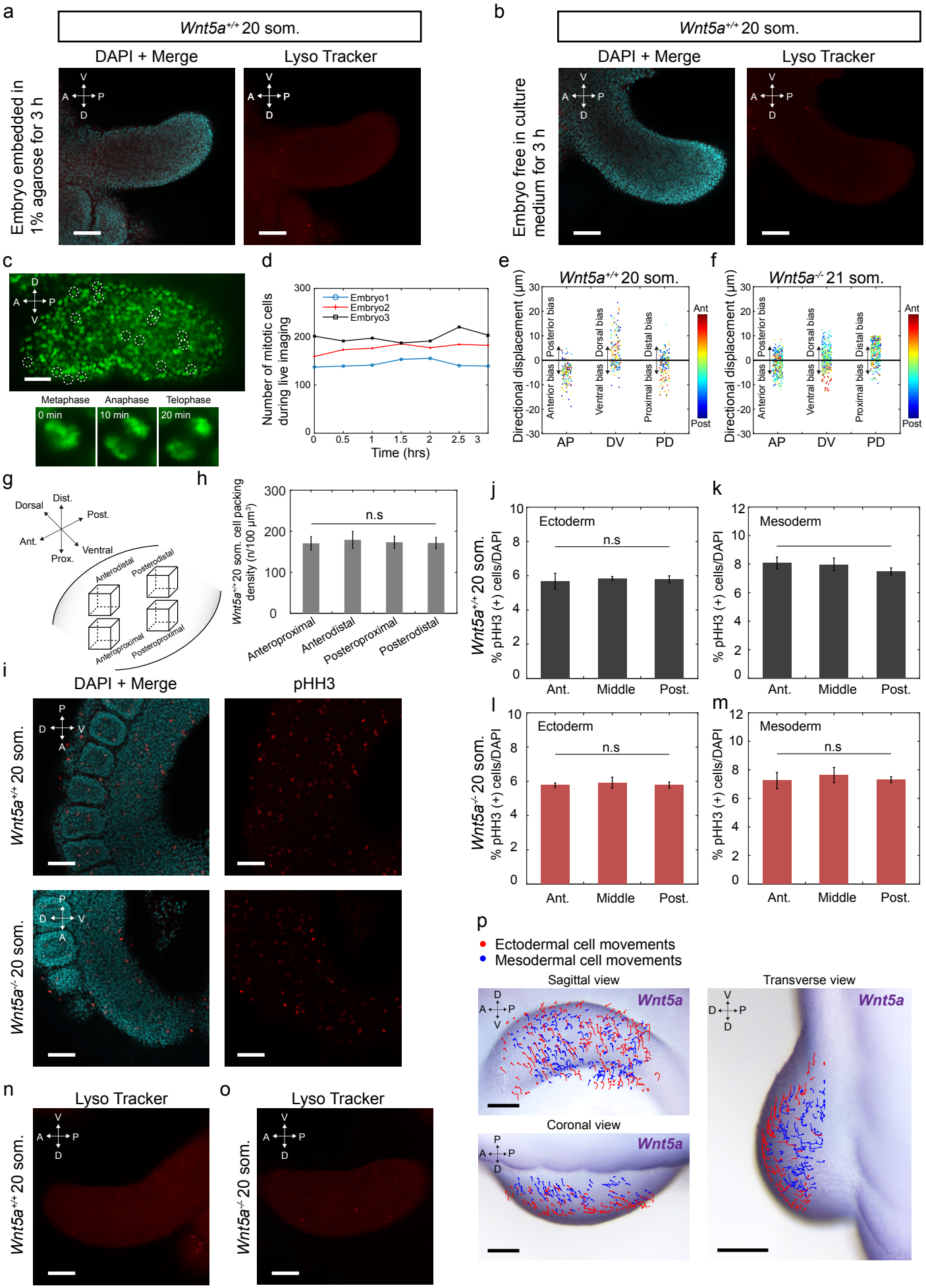

Figure S6. Collective cell migration contributes to early limb bud shape change but is not oriented towards the *Wnt5a* expression domain. a, b, Confocal images of 20 somite WT limb buds after 3h embedding in 1% agarose (a) and 3 h free in culture medium (b). In a, b, LysoTracker (red) and DAPI (cyan); scale bars: 100 μm. **c**, Light sheet image a 20 somite WT limb bud with *H2B-GFP* reporter. Circle-labelled are those cells undergoing mitosis. **d**, Number of mitotic cells in the limb bud field (20 somite WT embryos) over 3 h live imaging periods. **e**, **f**, Directional biases of cellular trajectories based on the 3D dandelion plots given in Figs. 3c and 3d are shown here along AP, DV, and PD limb bud axes for WT and *Wnt5a*$^{-/-}$ embryos. Cells are colour-coded based on their initial anteroposterior positions within the limb bud. **g**, Schematic depicting the four regions in which cell packing density was measured. **h**, Histogram representing cell packing density in locations shown in g (n=3 embryos). **i**, Confocal image of 20 somite WT and *Wnt5a* mutant limb buds visualising DAPI (cyan) and phospho-histone H3 (red). **j**-**m**, Histogram representing percentage of pHH3-positive cells in WT (ectoderm (j); mesoderm (k)) and *Wnt5a* mutant (ectoderm (l); mesoderm (m)) limb bud. **n, o,** Confocal image of 20 somite WT and *Wnt5a*$^{-/-}$ limb buds visualising LysoTracker (red). Scale bars represent 100 μm. **p**, Orthogonal views of cell tracks of a 21 som. embryo overlaid on images of a separate embryo showing the *Wnt5a* expression domain. Scale bars represent 50 μm.

Supplementary Figure S7

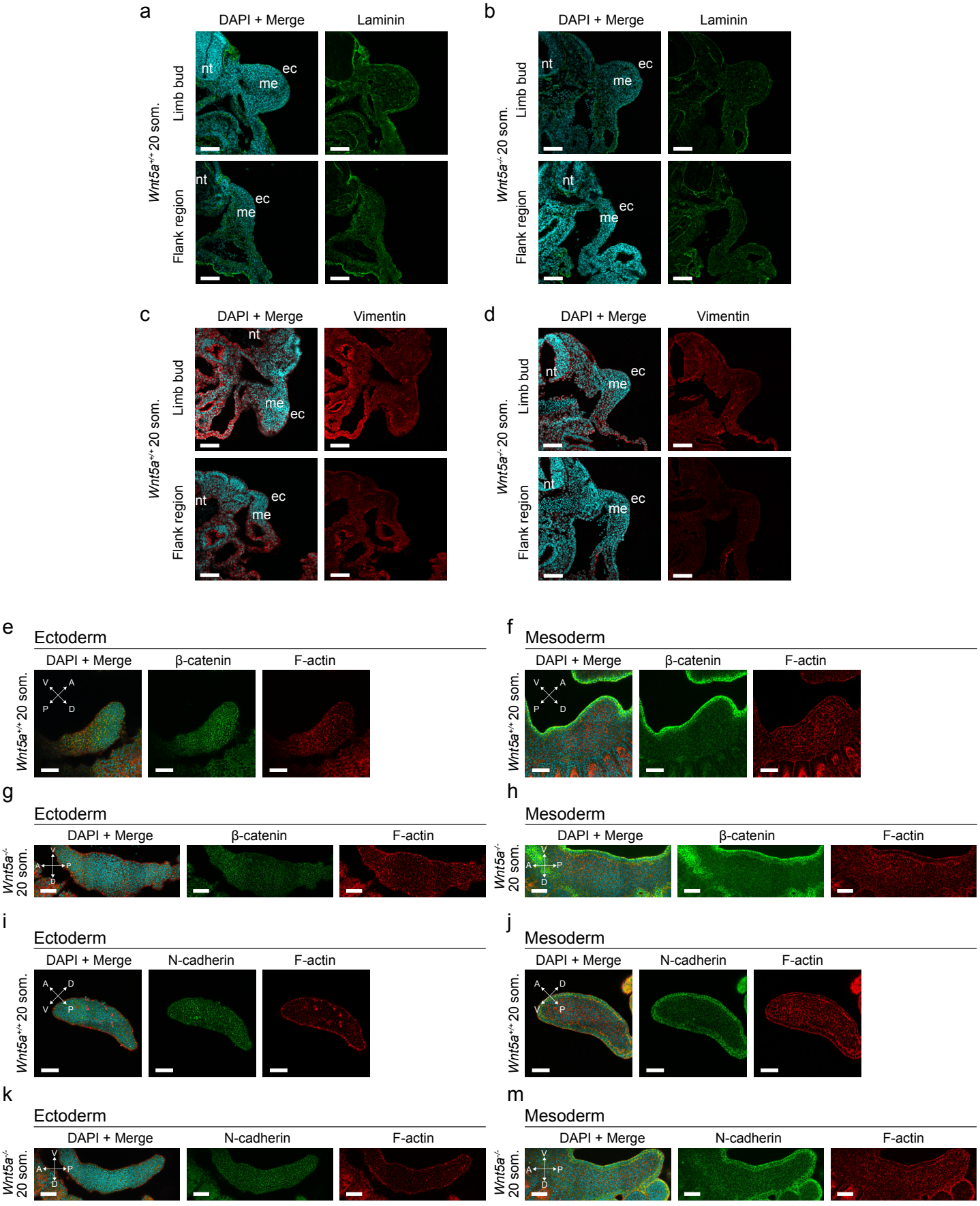

Figure S7. Immunostaining against ECM, cytoskeletal and cell-cell adhesion proteins within the limb field. a-d, Transverse sections of 20 somite WT (a, c) and *Wnt5a*$^{-/-}$ (b, d) forelimb and flank regions. Sections were stained with DAPI (cyan), anti-laminin antibody (green) and anti-vimentin antibody (red). **e-m**, Confocal sections of 20 somite WT (e, f, i, j) and *Wnt5a*$^{-/-}$ (g, h, k, m) limb buds visualising DAPI (cyan), F-actin (red), anti-β-catenin antibody (green in e-h) and anti-N-cadherin antibody (green in i-m). *n*=3 embryos for each condition. Scale bars represent 100 μm. nt, neural tube; me, mesoderm; ec, ectoderm.

Supplementary Figure S8

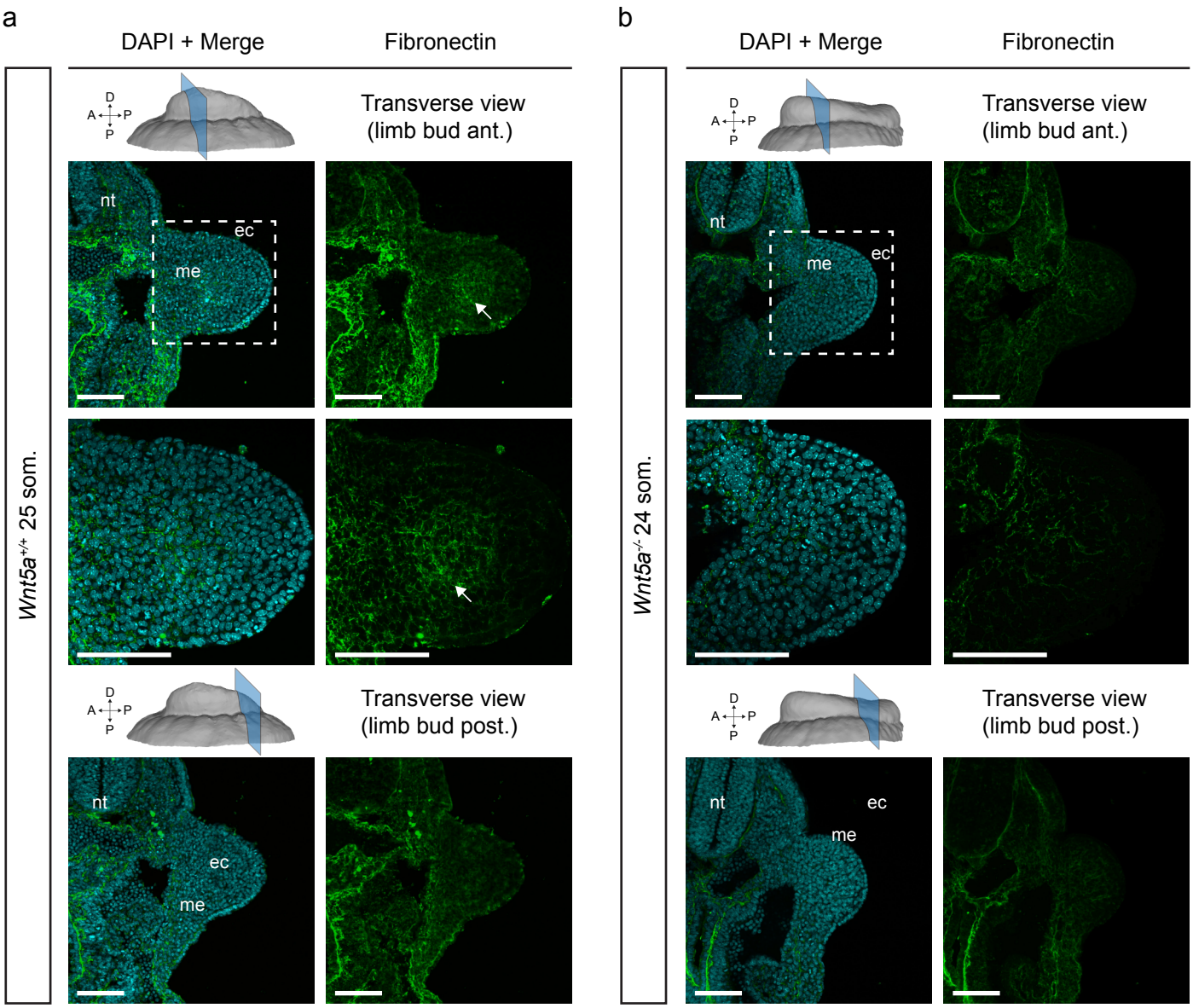

Figure S8. Fibronectin expression in 24-25 somite stage limb buds. a, **b**, Transverse and coronal sections of 24-25 somite WT (a) and *Wnt5a-/-* (b) embryos at forelimb anterior and posterior regions. Sections were stained with DAPI (cyan) and anti-fibronectin antibody (green). Arrows indicate the anteriorly biased region of fibronectin expression.

Supplementary Figure S9

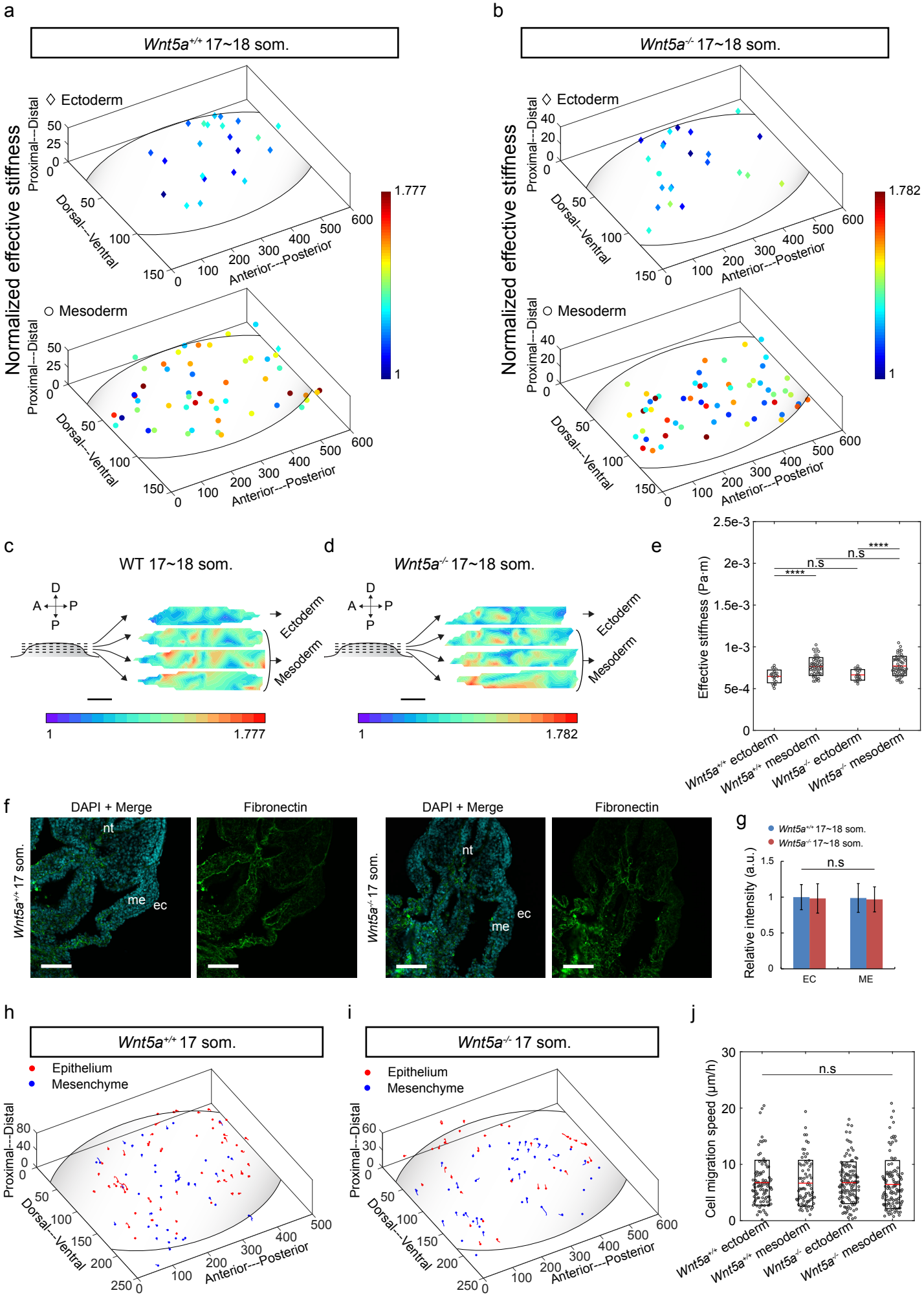

Figure S9. Stiffness gradient is absent and cell migration is diminished in 17-18 somite stage limb buds. a, b, Normalised effective stiffness maps of 17-18 somite WT (*n*=3 embryos) and *Wnt5a*$^{-/-}$ (*n*=3 embryos) limb buds. **c, d**, 3D rendering of the stiffness maps of a and b. **e**, Absolute effective stiffness values of data shown in a and b (two-tailed *t*-test, ****P<0.0001). **f**, Transverse sections of 17 somite WT and *Wnt5a*$^{-/-}$ limb buds. Sections were stained with DAPI (cyan) and anti-fibronectin antibody (green). **g**, Relative fluorescence intensity of fibronectin in 17 somite WT (*n*= 3 embryos) and *Wnt5a*$^{-/-}$ (*n*= 3 embryos) limb fields. **h, i**, 3D cell trajectories within 17 somite WT and *Wnt5a*$^{-/-}$ limb fields tracked from live light sheet time lapse Movies (unit: μm). Each dot denotes the last time point of tracking. **j**, Cell migration speed of 17 somite WT (*n*=3 embryos) and *Wnt5a*$^{-/-}$ (*n*=3 embryos) limb buds. Scale bars represent 100 μm. nt, neural tube; me, mesoderm; ec, ectoderm.

SUPPLEMENTARY TABLE S1

Comparison of effective stiffness (normalised by bead diameter for comparison) measured using different magnetic bead sizes within spatially matched limb bud regions of 20-21 som. embryos.

9.3 μm	Bead1	Bead2	Bead3	Bead4	Bead5
Deviation in comparison with corresponding 2.8 μm bead measured result	+8.77%	-5.88%	+12.17%	+6.77%	+2.35%

32 μm	Bead1	Bead2	Bead3
Deviation in comparison with corresponding 2.8 μm bead measured result	+9.13%	+10.99%	+7.32%

SUPPLEMENTARY MOVIE LEGENDS

Movie S1
Three dimensional normalised effective stiffness distribution within 20-21 somite stage WT limb bud. Circles and diamonds represent mesodermal and ectodermal measurements, respectively. Position 0 of the AP, DV and PD axes reflects anterior, dorsal and proximal respectively.

Movie S2
An continuous stiffness map of the 20-21 somite stage WT limb bud based on Delaunay triangulation between data points.

Movie S3
Three dimensional normalised effective stiffness distribution of 20-21 somite stage *Wnt5a*$^{-/-}$ limb bud. Circles and diamonds represent mesodermal and ectodermal measurements, respectively. Position 0 of the AP, DV and PD axes reflects anterior, dorsal and proximal respectively.

Movie S4
Three dimensional rendering and time lapse movie of a 20 somite *CAG::H2B-GFP* (WT) transgenic embryonic limb bud imaged by light sheet microscopy. Anterior is to the left, dorsal is upwards.

Movie S5
Three dimensional rendering and time lapse movie of a 21 somite *CAG::H2B-miRFP703* (WT) transgenic embryonic limb bud imaged by light sheet microscopy. Anterior is to the left, dorsal is upwards.

Movie S6
Three dimensional migration trajectories of a subset of cells of a 20 somite *CAG::H2B-GFP* (WT) transgenic embryonic limb bud imaged by light sheet microscopy. Blue and red tracks represent mesodermal and ectodermal cell movements, respectively. Position 0 of the AP, DV and PD axes reflects anterior, dorsal and proximal respectively.

Movie S7
Three dimensional rendering and time lapse Movie of a 21 somite *CAG::H2B-GFP;Wnt5a*$^{-/-}$ transgenic embryonic limb bud imaged by light sheet microscopy. Anterior is to the left, dorsal is upwards. The limb bud is in the centre (not the brighter region in the lower left of the frame). The counter in the lower right denotes 12 time steps at 10 min. intervals.

Movie S8
Three dimensional migration trajectories of a subset of cells of a 21 somite *CAG::H2B-GFP;Wnt5a*$^{-/-}$ transgenic embryonic limb bud imaged by light sheet microscopy. Blue and red tracks represent mesodermal and ectodermal cell movements, respectively. Position 0 of the AP, DV and PD axes reflects anterior, dorsal and proximal respectively.

Movie S9
Three dimensional normalised effective stiffness distribution within 17 somite stage WT limb bud. Circles and diamonds represent mesodermal and ectodermal measurements, respectively. Position 0 of the AP, DV and PD axes reflects anterior, dorsal and proximal respectively.

Movie S10
Three dimensional normalised effective stiffness distribution of 17 somite stage *Wnt5a*$^{-/-}$ limb bud. Circles and diamonds represent mesodermal and ectodermal measurements, respectively. Position 0 of the AP, DV and PD axes reflects anterior, dorsal and proximal respectively.

Movie S11
Three dimensional rendering and time lapse Movie of a 17 somite *CAG::H2B-GFP* (WT) transgenic embryonic limb bud imaged by light sheet microscopy. Anterior is to the left, dorsal is upwards.

Movie S12
Three dimensional migration trajectories of a subset of cells of a 17 somite *CAG::H2B-GFP* (WT) transgenic embryonic limb bud imaged by light sheet microscopy. Blue and red tracks represent mesodermal and ectodermal cell movements, respectively. Position 0 of the AP, DV and PD axes reflects anterior, dorsal and proximal respectively. The counter in the lower right denotes 12 time steps at 10 min. intervals.

Movie S13
Three dimensional rendering and time lapse Movie of a 17 somite *CAG::H2B-GFP;Wnt5a*$^{-/-}$ transgenic embryonic limb bud imaged by light sheet microscopy. Anterior is toward the upper left, dorsal is towards the upper right. The limb field is in the central, relatively dark part of the frame. The counter in the lower right denotes 12 time steps at 10 min. intervals.

Movie S14
Three dimensional migration trajectories of a subset of cells of a 17 somite *CAG::H2B-GFP;Wnt5a*$^{-/-}$ transgenic embryonic limb bud imaged by light sheet microscopy. Blue and red tracks represent mesodermal and ectodermal cell movements, respectively. Position 0 of the AP, DV and PD axes reflects anterior, dorsal and proximal respectively.